Analysis of Luminescence Quenching on Calf Thymus DNA

L. S. Schulman,*,† S. H. Bossmann,‡,§ and N. J. Turro§

Physics Department, Clarkson University, Potsdam, New York 13699-5820, Lehrstuhl für Umweltmesstechnik, Universität Karlsruhe, 76128 Karlsruhe, Germany, and Chemistry Department, Columbia University in the City of New York, New York, New York 10027

Received: September 22, 1994; In Final Form: February 28, 1995[⊗]

A new model for the calculation of DNA-mediated (long-range) photoinduced electron transfer is presented. This model uses a phenomenological approach to describe the interaction of photodonor and electron acceptor metal complexes in the presence of DNA and permits the calculation of characteristic interaction distances for the electron transfer between DNA intercalated species. The binding of two types of metal complexes to DNA is described probabilistically and the density calculation of the complexes on DNA is performed according to a random deposition model on a one-dimensional surface. The displacement of one complex species by the other at higher loading densities and the possible formation of supramolecular species between different metal complexes in solution or at the surface of DNA have also been considered. A fit of experimental data employing photoexcited $[Ru(phen)_2(dppz)]^{2+}$ as electron donor and $[Rh(phi)_2(phen)]^{3+}$ as electron acceptor has been performed. Using the model presented here, the experimental results are consistent with DNA-mediated long-range electron transfer occurring over a center-to-center distance of 24 Å.

Introduction

Can DNA serve as a medium that supports (long-range) electron transfer? This issue is of great importance for the understanding of the biochemical properties of DNA, especially in vivo DNA-damaging and DNA-damage repair reactions and for the development of efficient anticancer drugs.[1] The ability of DNA to support (long-range) electron transfer has been suggested several times,[2] but until recently compelling experimental evidence has been lacking.[3] The quantitative description of DNA-mediated electron transfer reactions can be regarded as key to the understanding of its working principles.

Recent investigations employing DNA-mediated electron transfer have involved the strong DNA intercalators bis(1,10-phenanthroline)(dipyridophenazine)ruthenium(II), $[Ru(phen)_2(dppz)]^{2+}$, as photoelectron donor and bis(9,10-phenanthrenequinone diimine)(1,10-phenanthroline)rhodium(III), $[Rh(phi)_2(phen)]^{3+}$, as electron acceptor.[3] Both complexes are avid binders to DNA with[4] $K_b > 10^6\ M^{-1}$, and their strong intercalation in DNA has provided results that are consistent with long-range electron transfer.[3]

$[Ru(phen)_2(dppz)]^{2+}$ exhibits no luminescence from water solution, but shows an intense luminescence if it is bound to DNA. Therefore, direct observation of the quenching reaction of the photoexcited and DNA-bound ruthenium complexes $(Ru(phen)_2(dppz))^{2+*}$ by $[Rh(phi)_2(phen)]^{3+}$ is possible in this special biochemical system.[4a]

The chemical structure of the donor–acceptor metal complexes is presented in Figure 1. Calf thymus DNA has been employed in the photoelectron electron transfer quenching experiments.

We present a quantitative model to examine DNA-mediated (long-range) electron transfer between metal donors and acceptors such as Ru and Rh–diimine complexes. We develop a phenomenological approach, not relying on detailed assumptions.

For instance, the well-known work by McGhee and von Hippel[5] considers "noncooperative and cooperative binding of large ligands to a one-dimensional homogeneous lattice". Further development of their work relies[6] heavily on the assumption of equilibrium conditions during the binding of (metal–complex) ligands to DNA. The equilibrium assumption seems to be reasonable for weak intercalators in DNA, as they are represented by the M(II)/(III)–tris(phenanthroline) family.[7] Nevertheless, in that case the electron transfer can occur over two pathways: (1) through the medium itself and (2) through motion and diffusion on the surface of DNA; thus extraction of information about the electron transfer properties of DNA derived from this approach is ambiguous.

The equilibrium assumption seems not to be valid in the case of two strong DNA intercalators as used in the studies described above,[3] an experimental system which provides substantial evidence for DNA-mediated long-range electron transfer.

Therefore, a nonequilibrium assumption in combination with a time-dependent displacement and ordering mechanism of strongly intercalating metal complexes at the DNA double strand appears to be an appropriate way to develop a theory of DNA-mediated long-range electron transfer reactions. We note too that, although the curves developed in our phenomenological model at times resemble those of McGhee and von Hippel, our approach has the advantage of making clear that curves of this sort are more general than any particular model (in particular those curves that rely on equilibrium assumptions).

In this report we will develop a basic and relatively simple model for the description of electron transfer reactions between intercalated donor–acceptor couples using calf thymus DNA (B-DNA) as medium.[8] As mentioned above, $[Ru(phen)_2(dppz)]^{2+*}/[Rh(phi)_2(phen)]^{3+}$ bound to calf thymus DNA serves as the test system. The experimental data obtained from ref 3 will be fitted. In a separate publication we will develop a description for the interaction of intercalated donor–acceptor couples as a function of the length of the DNA double strand.

A long-range goal of our modeling is the development of a systematic solution for DNA-mediated electron transfer, including the equilibrium and the nonequilibrium cases, in one theoretical framework. In this context, which is a rather general

† Clarkson University.
‡ Universität Karlsruhe.
§ Columbia University in the City of New York.
⊗ Abstract published in *Advance ACS Abstracts,* May 15, 1995.

0022-3654/95/2099-9283$09.00/0

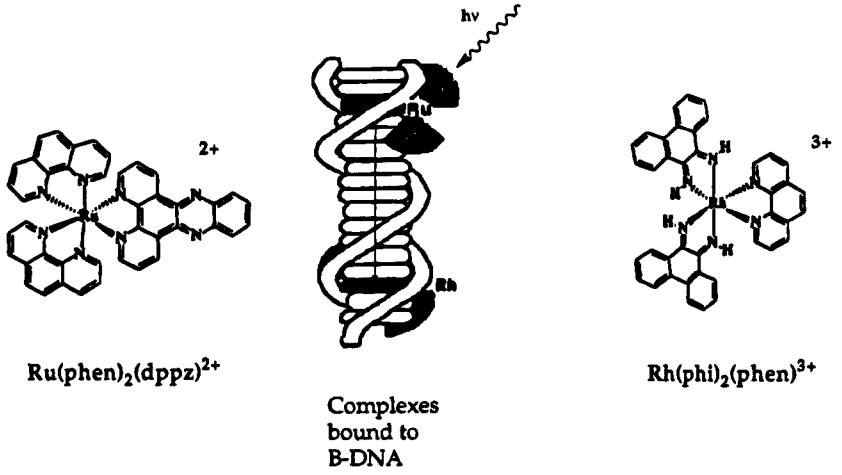

Figure 1. Structures of the complexes $[Ru(phen)_2(dppz)]^{2+}$ and $[Rh(phi)_2(phen)]^{3+}$ employed in the quenching experiments on B-DNA[3] which are fitted using the model presented here.

one, a comment on our methodology is in order. This comment should help in the interpretation of our results, especially the electron transfer distance. As indicated, our approach is phenomenological. This means that our main criterion in selecting fitting functions is simplicity, either in form or in mathematical tractability. The way we tested these functions (for example, the exponential assumed for the quenching versus distance relation or the on-strand density versus total density of complexes) is to change the form slightly and check that our results are relatively insensitive. We find that this gives us a robust understanding of the data. But this model-independence has its price. It means that one should treat our results with the same conceptual error bars that produced them. A case in point is the electron transfer distance, which for us played the role of a parameter L in the formula, $\exp(-n/L)$, that described the decline of quenching effect as the distance between electron donor and acceptor increased. We also attempted fits with sharp cutoffs (step functions) and inverse power laws. This had little effect on the quality of the fits, but it did involve different parametrization. Thus, the parameter used for a sharp cutoff does not have the same meaning as the exponential decay length, and in the absence of a full quantum mechanical theory of the quenching (which is why we are using phenomenology) there isn't a way to make a precise correspondence. Of course, with sufficiently comprehensive data one could attempt to choose between these fitting functions, and indeed this would be an important objective for understanding what does give rise to the electron distance we have found. Certainly, exponential, sharp cutoff, and power law, corresponding to different physical mechanisms, and with more comprehensive data the theory of this paper could be used to distinguish these dependencies. (As indicated, such use has already been made for casual comparison, but distinctions could not be justified with the available data.)

In light of these remarks, it should be noted that the figure we give (24 Å) for electron transfer distance is subject to all the caveats we have just stated for our phenomenology. It must also be emphasized that it is a *center-to-center* distance. For the *separation* distance of the complexes one should subtract half the diameter of each complex. For $[Ru(phen)_2(dppz)]^{2+}$ this diameter is roughly 16−10 Å (depending on orientation), and for $[Rh(phi)_2(phen)]^{3+}$ it is roughly 13−11 Å. Taking approximate values, this means that our electron transfer distance is perhaps 10 Å beyond actual contact. The conservative statement of our conclusions is thus that there is definitely quenching significantly beyond contact, but it would be foolish to insist that, for example, there must be a wave function whose tail drops off exponentially with this characteristic length.

Results and Discussion

1. Description of the Calculation Method. We use a phenomenological approach to provide a quantitative description of medium-mediated electron transfer. The specific system to be modeled is the DNA-mediated electron transfer quenching of intercalated sensitizers and electron acceptors. Quantities and effects of interest are the following: (a) the density of sensitizer (photoelectron donor) adsorbed on the DNA (symbolized in the schemes by circles or in the text by the symbol C); (b) the density of quencher (acceptors) adsorbed on the DNA (symbolized in the schemes by squares or in the text by the symbol S); (c) the consequences of incomplete absorption of both kinds of complex on the DNA strand; that is, some fraction of either complex remains in solution; (d) the characteristic drop-off length of the quenching effect; (e) the consequences of attraction or repulsion between C and S.

We derive quenching expressions which describe the quenching efficiency as a function of the factors a−e (in terms of parameters defining them). The two crucial issues, namely, the amount of complex in solution and the effect of S−C attraction, will be dealt with in a phenomenological way.

In the calculation it will be assumed that the quenching effect of an electron acceptor S on a particular photodonor C is independent of whether or not there are intervening C's along the strand. The alternative, having a C block the effect of S, can also be calculated, but is considered less likely to represent the physical situation.

1.1. Basic Formulas. For the computation, a number of parameters related to quantities and effects a−e are now defined: ϱ_c = density of DNA-bound sensitizers ("circles", C); ϱ_s = density of DNA-bound quenchers ("squares", S); $\varrho = \varrho_c + \varrho_s$ = total density of bound complexes; L = characteristic drop-off length of the quenching effect; I = normalized emission intensity (Stern−Volmer parameter) per circle = I/I_0; β, γ, R = parameters related to S−C interactions; ϱ_∞ = parameter determining relative amount of complex on the DNA and in solution.

The unit of length is the site exclusion factor of the square (S) or circle (C), both of which are conventionally taken to be four DNA base pairs in length. This assumption is derived from absorption and emission titrations[9] employing $[Ru(phen)_2(dppz)]^{2+}$ on CT-DNA, which have demonstrated the site-

exclusion effect of $[Ru(phen)_2(dppz)]^{2+}$ and $[Rh(phi)_2(phen)]^{3+}$ to be two base pairs on either side.[4e,f]

At this point of the model development the treatment ignores effects due to blocking, open gaps of length 1, 2, or 3 base pairs, etc. However, these effects will be accommodated below (see section 3).

2. First, Simplest, Derivation: No Correlations in Binding, All Complexes Bound to DNA. We begin by computing the Stern–Volmer parameter I according to the following simplifying assumptions: First, there are no correlations, positive or negative, in the locations of the S's and the C's on the strand. Secondly, as defined in section 1.2, all metal complexes put into solution bind to the DNA in one binding mode.

Consider a particular circle. Its environment will be estimated probabilistically. The total luminescence is the sum of individual luminescences. The equivalence of all sites (except for the negligible effect at the end points) justifies the assumption that the total luminescence I is a multiple of the individual site luminescences.

The environment of each donor–circle is characterized by the distance to the nearest quencher-square on its right and on its left. Let these distances be respectively denoted by m and n. According to our convention, m and n are measured in units of 4 base pairs.[10]

Let p_{mn} be the probability that the nearest square to the left is a distance m and the nearest square to the right a distance n. When there is minimal space between the circle and the nearest square, the distance n (or m) will be taken to be 0. Since at this stage we assume no correlations in the siting of C's and S's, the probabilities p_{mn} for the associated left and right environments are given by the following:

$$p_{mn} = \varrho_s^2(1 - \varrho_s)^{m+n} \tag{2.1}$$

The quenching of a single square at a distance n will assumed to be given by a factor $\exp(-n/L)$; that is, the quenching behavior is assumed here to follow an exponential drop-off with some characteristic length L. The effect of a single square (at distance n) will thus be taken to be a reduction of luminescence by a factor of $1 - \exp(-n/L)$. The luminescence reduction from the combined effect of two squares will be assumed to be the product of the luminescence reduction of each individually. Therefore, the intensity, $I(m,n)$, with squares at distances m and n from the circle is given by

$$I(m,n) = [1 - \exp(-m/L)][1 - \exp(-n/L)]$$

Thus, if a square on the left at distance 2 decreases luminescence by 70% (leaving 30% of the signal), then squares at distance 2 on both sides will leave only 9% (i.e., 30% squared) of the signal, for a quenching factor of 91%. We obtain the total signal intensity I by summing over all the possibilities for the condition of the given circle:

$$I = \sum_{m=0}^{\infty}\sum_{n=0}^{\infty} p_{mn} I(m,n)$$

$$= \sum_{m=0}^{\infty}\sum_{n=0}^{\infty} (1 - \varrho_s)^{m+n}\varrho_s^2[1 - \exp(-m/L)][1 - \exp(-n/L)] \tag{2.2}$$

Since the events to the left of the given circle are statistically independent of those to the right, the probabilities factor. However, the rule for combining luminescence does not have to respect this relation. Our assumption about combining the quenching effect as a product is what makes the formula relatively simple and thus permits the straightforward calculation of the total luminescence intensity. Relaxing this assumption should make little difference in the numerical solution, but it simplifies the analytical solution. It follows that

$$\sqrt{I} = \sum_{n=0}^{\infty}(1 - \varrho_s)^n\varrho_s[1 - \exp(-n/L)]$$

$$= 1 - \sum_{n=0}^{\infty}(1 - \varrho_s)^n\varrho_s \exp(-n/L)$$

$$= 1 - \frac{\varrho_s}{1 - (1 - \varrho_s)\exp(-1/L)} \tag{2.3}$$

This is our final expression for the simplest situation: no correlations between squares and circles and the density of squares put in solution is the density on the DNA.

We note that for the case of "blocking", namely, when an intervening circle suppresses the quenching of a square and circle on either side of it, the formula is similar. The only change is that in the denominator of the last expression ϱ ($=\varrho_s + \varrho_c$) replaces ϱ_s:

$$\sqrt{I} = \frac{\varrho_s}{1 - (1 - \varrho)\exp(-1/L)} \tag{2.4}$$

3. The Effect of Complexes Left in Solution. In reality, not all the complexes put in solution are bound to the DNA. Since an exact measurement of the fraction of sensitizers and quenchers intercalated into DNA has not yet been successfully performed, the approach to be used here will be phenomenological. A simple functional dependence of the DNA-binding behavior of both the donor and acceptor metal complexes on their total concentration will be assumed, and a parameter in that function will be varied to fit the data. We choose this route in preference to more elaborate theoretical calculations because the many assumptions in such calculations are difficult to justify, so that a fit may lead to a false sense of comprehension, whereas it is merely a more elaborate form of phenomenology.

In particular, in considering whether we could use the McGhee–von Hippel methodology,[5] we are skeptical as to whether the equilibrium assumption applies for strongly binding metal complexes to DNA, at least within the time during which a typical photophysical experiment (steady state quenching, laser-flash, SPC) is performed.[11] Moreover, in dealing with interspecies interactions (possible attractive C–S forces in our case) a theory based on their interaction model has not yet been developed. Another intrinsic danger to keep in mind is that it is inappropriate to make too many claims from data that are limited in quantity and precision.

The intuitive physical picture is that at low concentrations essentially all metal complexes put into solution bind to the DNA, while for larger concentrations ("loading") the fact that many sites are occupied makes it increasingly difficult for more of them to bind to the DNA. This consideration is especially important in the case of intercalation as the main binding mode. Partly this will be due to the effects calculated in the McGhee–von Hippel model,[5] where one envisions an equilibrium between free complexes and free sites with bound complexes, and that equilibrium is governed by a finite association constant or affinity. But there will be other effects, for example, a weakening of the intrinsic binding strength as the DNA strand's properties are changed with increasing loading. Another issue is the possibility of a slow equilibration expected for high

SCHEME 1[a]

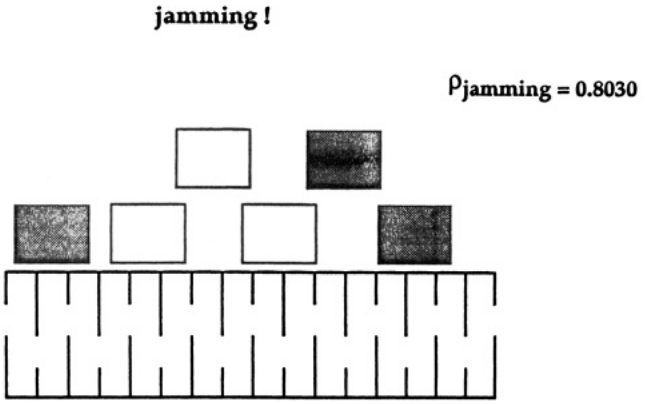

[a] The maximum density of complexes on DNA is limited in the case of nonequilibrium and random deposition. Unfillable spaces of size 1, 2, and 3 (base pairs) form because of either irreversible attachment or a steady state equilibrium situation with a slow exchange mechanism. The value ϱ_{jamming} is associated with $K = \infty$ or the "car parking limit", ref 12.

loading. In strongly bound complexes one expects configurations resembling those of random sequential absorption.[12] The influence of random sequential absorption—consistent with the nonequilibrium condition during the binding process—is shown schematically in Scheme 1 for absorption of a single species (i.e., S).

Because of the above concerns, we employ a phenomenological fit of the following form:

$$\tilde{\varrho} = \frac{\varrho}{1 + (\varrho/\varrho_\infty)} \tag{3.1}$$

where $\tilde{\varrho}$ is the "true" density of complexes (both S and C) actually bound on the DNA. The notation for the newly introduced parameter ϱ_∞ is based on the limiting value of $\tilde{\varrho}$ as $\varrho \to \infty$. We will assume that ϱ_c and ϱ_s are equally affected by these considerations. This assumption may be incorrect and relates to the issue of "displacement" of squares by circles. In calculations not reported here we have explored alternative assumptions but did not find substantially different conclusions. It is possible that for short strands (e.g., a synthetic DNA-28-mer) this issue will prove important and the matter will be reopened when we deal with them.

The form of eq 3.1 has the desired property $\tilde{\varrho} \sim \varrho$, for small ϱ, while for high loading the reduction may be considerable, depending on the adjustable parameter ϱ_∞.

We next discuss the fact that the complexes are of size 4 (measured in base pairs). This affects our calculation in two ways: First, when we set "distance" equal to an integer multiple of 4 base pairs, we ignore the finer gradations of quenching that would arise from complexes at distances that are not multiples of 4 base pairs. We assume that this effect is not significant and would only become significant if our claimed precision for L, the quenching range, would be on the order of 1 base pair (i.e., 1/4 in our units) or if L were so small that direct, or almost direct, contact between sensitizer and quencher on DNA would be required to permit electron transfer quenching. The other major effect of the length-4 property is the fact that as the strand fills, there are many unfillable gaps (of length 1, 2, or 3 base pairs) so that the maximum density is less than that for dense packing. In fact there is considerable research on the nonequilibrium, extremely high affinity case, known as random sequential absorption or the "car parking problem". It is known[12,13] that dropping length-4 objects on a linear lattice, and letting them stick where they land, has an asymptotic jamming density of about 0.80 (see Scheme 1). With finite adhesion this limit can be exceeded. Because of our displacement hypothesis, the density of squares and circles actually on the strand will be assumed to be proportional to their overall density. Thus,

$$\tilde{\varrho}_c = \varrho_c \frac{\tilde{\varrho}}{\varrho} \qquad \tilde{\varrho}_s = \varrho_s \frac{\tilde{\varrho}}{\varrho} \tag{3.2}$$

It should also be pointed out that even with this selection of a value for ϱ_∞ we do not have a unique phenomenology. This is because other functional forms for the dependence of $\tilde{\varrho}$ on ϱ, having the same small and large ϱ asymptotics, such as

$$\tilde{\varrho} = \varrho_\infty[1 - \exp(-\varrho/\varrho_\infty)] \tag{3.3}$$

may be used in place of (3.1). Although we do not have a theoretical preference for one or the other form, (3.3) gave generally inferior fits to the experimental data. (However, when displacement was not allowed and blocking assumed, the form (3.3) gave reasonable results.) The essential reason for preferring (3.1), though, is simplicity, in the following sense. Although we constrain our functional forms to have the correct large ϱ asymptotics, our experimental situation is that we have a well-understood relation at low ϱ and want to extend beyond that regime with a minimum of artificial assumptions. As such, we seek an expression that involves the lowest possible powers of ϱ. It is (3.1) that does this.

4. Effect of Attraction between Complexes. We now examine the effect of attraction between complexes. In this section we describe the phenomenology used. In section 5 we will discuss alternative approaches, including the relationship of this work to that of McGhee and von Hippel.[5]

The quantity needed for luminosity calculations is ϱ_n, the probability of having a square n places to the right of a particular given circle, with no intervening squares. If the left- and right-side distributions are independent, this will be enough information to develop a model for the computation of p_n. Ideally, one would like a model, for example, giving relative S and C binding strengths (or chemical potentials) and a net attractive energy between them and deduce from this p_n. Instead, we will postulate the form of the distribution function itself and use a natural parametrization to fit the data, allowing for some level of attraction. In this more modest approach, one ultimately aims to relate this parametrization to experimental quantities.

Experimentally,[3,4] there were no indications for the formation of ground state or excited state supramolecular species from $[Ru(phen)_2(dppz)]^{2+}$ and $[Rh(phi)_2(phen)]^{3+}$ in the presence of DNA or in ethanol. No changes in the absorption or emission spectra of both complexes have been detected, except for a loss in the luminescence intensity of $[Ru(phen)_2(dppz)]^{2+}$ in the presence of $[Rh(phi)_2(phen)]^{3+}$. Therefore, for the particular experiments[3,4] that we are now addressing, it would not be justified to explain the observed high quenching in the presence of DNA[3,4] by the formation of donor—acceptor pairs. However, the formation of supramolecular species cannot be excluded in general and should be considered to be a competing quenching process in a universal model for electron transfer quenching through DNA.

In studying the gap distribution function, p_n, we handle the terms p_0, and p_n, $n \geq 1$, separately. This reflects possible short-range attractive interactions of the two species of the complex. To p_0 we assign a number γ_0. For the others we assume a form similar to that for noninteracting particles, namely, the distribution whose two-square version is given in eq 2.1. Thus, $p_n \sim$

SCHEME 2[a]

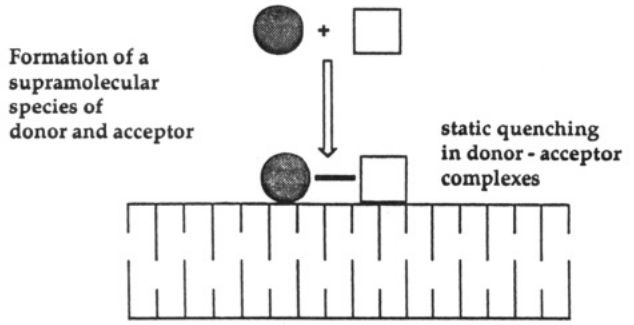

[a] Equations 4.1−4.6 for the case in which $R > 1$ could be the result of the formation of a supramolecular species of donor and acceptor on the DNA surface. This process would lead to the formation of additional close encounters and results in stronger static quenching. No evidence was found for this.

$\gamma_1(1-\gamma_1)^{n-1}$ with γ_1 an additional parameter. (The choice "$n-1$", rather than n, as the exponent is arbitrary and is adopted for later convenience.) Since $\sum_0^\infty p_n = 1$, the overall size of p_n for $n \geq 1$ is fixed and we have

$$p_n = \begin{cases} \gamma_0 & \text{for } n = 0 \\ (1-\gamma_0)(1-\gamma_1)^{n-1}\gamma_1 & \text{for } n \geq 1 \end{cases} \quad (4.1)$$

Observe that the form (4.1) can be reached in a variety of other ways. It is obtained for the equilibrium distribution of a single-species self-interacting lattice gas (equivalent to the Ising model) and is also the form postulated by McGhee and von Hippel.[5] Note, however, that these are *single*-species calculations, and, as we remark below, the latter reference does not deal with the multispecies interacting case.

We wish, nevertheless, to emphasize that although eq 4.1 seems entirely reasonable, it is not the only possibility, for example, if the enhancement of p_0 took place not through preferred attachment from solution but rather through diffusion of complexes already attached to the strand. Then one might expect a depletion of p_1 and enhancement of p_0, while the other gap probabilities retained their values, namely, $\varrho_s(1-\varrho_s)^n$ (for $n \geq 2$). This cannot be written in the form (4.1). A complete theoretical understanding would involve dealing with the issues of multiple species, variable attachment constants, interactions between the species, nonequilibrium, and diffusion.

The relatively simple description of the possible (supramolecular) interaction of photodonors and electron acceptors presented here is shown in Scheme 2.

There is the further matter of changes in the properties of the DNA as loading is increased (changing parameters for the foregoing considerations). To our knowledge no theory to describe such changes currently exists, although one might envision Monte Carlo simulations even for this level of complexity. In any case, in the present paper our preference is to seek phenomenological fits.

Because of the overall constraints on the number of squares and circles, the interaction parameters γ_0 and γ_1 *do not represent two independent parameters*. However, their exact relation to ϱ_s and ϱ_c depends on additional properties of the distribution of complexes. We will arrive at a relation in a way that should be robust for small ϱ_c or if the difference between γ_0 and γ_1 is not too great (and which is yet more reliable if both these properties are true, as for the experiments[3,4] that we study here).

Let us examine the relation between ϱ_c, ϱ_s, γ_0, and γ_1, by imagining that the C's are laid down first with density ϱ_c. In each remaining position an attempt is made to put a square. This attempt is successful with probability β_0 when the site has a C as a neighbor, β_1 when it does not. With this scheme the gap distribution is calculated as follows: To have a gap of size zero—by convention, to the right of a given circle—means that the site to the right of the circle is, firstly, not occupied by another circle and, secondly, it is occupied by a square. The probability of this is $\beta_0(1-\varrho_c)$. The existence of a gap of size n, with $n \geq 1$, requires that the attempts to fill the first and next $n-1$ sites fail and that the attempt to fill the $(n+1)^{st}$ succeed. The probability of a gap of size n therefore is

$$[1-(1-\varrho_c)\beta_0][1-(1-\varrho_c)\beta_1]^{n-1}(1-\varrho_c)\beta_1 \quad (4.2)$$

There is an approximation implicit in eq 4.2. Because we are asking for the first S, irrespective of the appearance of a C within the "gap", it is possible that for some of the intermediate terms β_0 should be used in the above expression in place of β_1. This effect will be small if β_0 and β_1 do not differ by much. It will be small if ϱ_c is small. It will also be less important at high loading (large ϱ_s) since gaps will be smaller. For the experiments discussed in this article $\varrho_c = 0.08$; coupled with the expectation of relatively small interaction effects, this justifies the use of eq 4.2.

Comparing the probabilities just derived from the stochastic formation model with the expressions in eq 4.1, we make the identifications

$$\gamma_0 = (1-\varrho_c)\beta_0 \qquad \gamma_1 = (1-\varrho_c)\beta_1 \quad (4.3)$$

To relate ϱ_s to β_0 and β_1, we need to know the number of gaps of size k separating the C's, after they have been laid down. Call this quantity n_k. The expected number of gaps of size k is the number of C's times the probability that a given C has a gap of size k to its right. The latter probability is something we have already calculated in the simpler case of no interaction. It follows that $n_k = (N\varrho_c)\varrho_c(1-\varrho_c)^k$.

Using n_k we deduce the number of squares as follows: Each gap of size 1 has a probability β_0 of having an S in it. Gaps of size 2 have an expectation value $2\beta_0$ for S occupation. For gaps of size 3 or more the interior sites have a probability β_1 of occupation. Therefore, the expected occupation of size-k gaps is $2\beta_0 + (k-2)\beta_1$, with this formula holding for the case $k = 2$ as well as for $k > 2$. The total expected number of squares is therefore given by

$$\text{number of squares} = N\varrho_s$$

$$= n_1\beta_0 + \sum_{k=2}^{\infty} n_k[2\beta_0 + (k-2)\beta_1] \quad (4.4)$$

Doing the sum in (4.4) and replacing the β's by γ's (using (4.3)), we obtain

$$\varrho_s = \gamma_1 + (\gamma_0 - \gamma_1)\varrho_c(2-\varrho_c) \quad (4.5)$$

The above relates γ_0 and γ_1 to ϱ_s, but it is convenient to replace them by more immediately interpretable expressions. First, we define $R \equiv \gamma_0/\gamma_1$. This is a measure of the interaction. Values of R greater than 1 represent attraction. Substituting in eq 4.5, we have for γ_1

$$\gamma_1 = \frac{\varrho_s}{1+(R-1)\varrho_c(1-\varrho_c)} \quad (4.6)$$

This expression can then be substituted in (4.1) to obtain the gap distribution function in terms of ϱ_s and a single parameter measuring the attraction, R. This parameter is analogous in some ways to the "ω" of McGhee and von Hippel[5] but because

SCHEME 3[a]

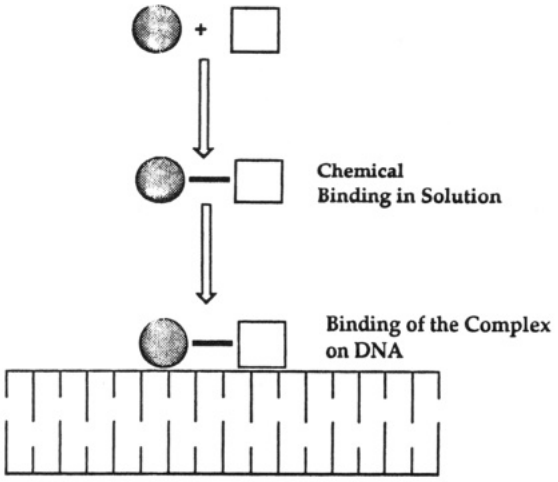

[a] In section 5.2, we describe the formation of a "real" complex between one donor and one acceptor molecule in solution. The previously formed complex then drops on DNA. Again, no evidence was found for this process.

of the different context (multispecies, nonequilibrium, etc.) cannot be identified with their "ω". Note too that R does not affect the relative amount of substance on or off the strand, only its distribution on the strand. This is because γ_0 and γ_1 are normalized to a given amount of on-strand complexes, the latter quantity affected only by ϱ_∞, among our parameters.

The expressions derived here will be used below (section 6) to obtain the luminosity as a function of loading.

Finally, we point out one further approximation involved in our derivation (which we prefer to think of as the motivation for a particular phenomenological expression). For simplicity we assumed that the C's were laid down and the S's found their way among them. This is probably not true, and in calculating the amount of material on the DNA and the amount remaining in solution we treat C's and S's equivalently. This is the "displacement" assumption. Although for the low C densities with which we work this should make little difference, one should be aware of this approximation if one goes to higher C densities.

5. Discussion of Other Methods for Dealing with Interactions between Metal Complexes. *5.1. The Method of McGhee and von Hippel.*[5] For two reasons the method of McGhee and von Hippel[5] does not appear to apply to the problem at hand. First, as we have already remarked, the equilibrium assumption on which their method is based seems not to apply to our situation. Secondly, for the more complex case of interacting—attracting or repelling—species, a possibility that we explicitly wish to consider, their method has not been developed. Furthermore, as they remark[5] (p 486), the "simple conditional probability approach may founder". In effect what one needs is a multicomponent lattice gas, equivalent to a one-dimensional Potts model.[16] Although algebraically complex, such a system could be successfully studied if one were dealing with an equilibrium problem.

We remark, however, that from the standpoint of curve parametrization the functional dependence of the gap distribution function (eq (4.1)) is the same as the McGhee–von Hippel single self-interacting species gap distribution function.[5] The reason is that the (short-range interaction) and (Poisson distribution beyond that) assumptions allow a limited class of distribution functions. This coincidence illustrates the danger of taking any particular theoretical framework too literally. One might have believed a successful data fit (with blind use of the McGhee–von Hippel formalism) to be a confirmation of the equilibrium assumption, whereas all it represents is the limited possibilities for simple phenomenological fitting functions.

5.2. Chemical Bonding of S's and C's. Although we do not believe there to be supramolecular interactions between C's and S's, we briefly present a model in which the effect of such binding could be included. In practice, it was the use of this model—and the fact that the data were well fit without it—that allowed us to discard it.

Suppose that the DNA-attached circles and squares may interact and bind to each other. Rather than attack the full dynamical problem, including binding and unbinding on the DNA, we use a simplified picture of the effect of possible S–C attraction. Scheme 3 shows the mechanistic picture. We assume that the attraction causes formation of S–C pairs (called "P") and that these three species are in equilibrium. In the context of reaction theory we use a slightly different notation: [C] = density of circles ($=\varrho_c$), [S] = density of squares ($=\varrho_s$), and [P] = density of pairs. The reaction is C + S $\rightleftharpoons$ P. By the law of mass action, there is a constant β such that [P] = β[C][S]. In addition, the following quantities are constant and equal to their initial values:

$$[S] - [C] = [S_0] - [C_0],\ [C] + [S] + 2[P] = [S_0] + [C_0] \quad (5.1)$$

where the 0 subscripts refer to initial values, and the unsubscripted quantities to the equilibrium values.[17] By straightforward algebra one obtains the following:

$$[C] = [-(1 + \beta y) + \sqrt{1 + \beta^2 y^2 + 2\beta x}]/(2\beta) \quad (5.2)$$

where $x \equiv [S_0] + [C_0]$ and $y \equiv [S_0] - [C_0]$.

In practice it turned out that varying β did little to improve the fits to the data and that, as we pointed out earlier, no experimental evidence[3,4] was found for the formation of a supramolecular species in the experiment here under consideration. Therefore, further theoretical refinements along this line will not be pursued in this publication.

5.3. Ising Model for a Lattice Gas. As mentioned above, if equilibrium prevailed, a consistent method for handling this problem would be a one-dimensional Potts model (or, equivalently, a multispecies lattice gas).[16] If the real size of the complexes, which are definitely larger than the amount of space for one DNA base pair, is neglected, one has a three-state model (S, C, or ∅ (empty site)) and a variety of particle–particle couplings can be accommodated. Also, by varying the chemical potential for S's and C's, one could effectively deal with the varying number of squares or circles that actually bind to the DNA double strand under various circumstances. The gap distribution function, p_n, can then be calculated in a straightforward, if tedious, way. This may prove necessary for dealing with short strand problems, where different bonding of S and C to the strand may play a significant role.

For the analysis of the results of electron transfer between complexes bound to calf thymus DNA, the use of this model is not warranted by the data. Recall too that this approach is only valid in equilibrium.

6. Combined, Comprehensive Calculation. The actual data fit was made using eqs 2.3, 3.1, 3.2, 4.5, and 4.6, and represent a comprehensive phenomenological treatment. It is our view that this is warranted both by the data and by the absence of any systematic theory.

Since the fitting procedure is not quite a matter of substituting successive quantities in successive equations, we review the steps. In principle we should go back to (2.2), but since left

and right sides of our given circle are still independent and since we still assume the factoring of the quenching effect, we start directly with eq 6.1.

$$\sqrt{I} = \sum_{n=0}^{\infty} p_n(1 - \exp(-n/L)) \tag{6.1}$$

For the gap distribution function in eq 6.1 we use the expression 4.1 with γ_0 given by $\gamma_0 = R\gamma_1$, and γ_1 expressed in terms of ϱ_s, etc., by eq 4.6:

$$\gamma_1 = \frac{\varrho_s}{1 + (R-1)\varrho_c(1-\varrho_c)} \tag{4.6, 6.2}$$

Performing the relevant sums, the square root of the luminosity (as in eq 2.3) is

$$\sqrt{I} = 1 - \frac{\gamma_1[R - \alpha(R-1)]}{1 - \alpha(1-\gamma_1)} \tag{6.3}$$

with

$$\gamma_1 = \frac{\varrho_s}{1 + (R-1)\varrho_c(1-\varrho_c)} \quad \text{and} \quad \alpha = \exp(-1/L) \tag{6.4}$$

We next include the fact that the densities to be used do not reflect the total amount of material in solution, but only that on the DNA double strand. In section 3 these quantities were marked by tildes, so that from (3.1) and (3.2) we have

$$\tilde{\varrho}_s = \frac{\varrho_s}{1 + (\varrho/\varrho_\infty)} \qquad \tilde{\varrho}_c = \frac{\varrho_c}{1 + (\varrho/\varrho_\infty)} \tag{6.5}$$

For the final form for the quenching we include one additional factor that we have heretofore not mentioned. Because the amount of C on the strand is a function of ϱ_s (through (6.4)), the addition of S's to the solution reduces the luminosity simply by pushing C's off the strand. Since we normalize our quenching factor with respect to zero loading ($\varrho_s = 0$), it is convenient to write $\tilde{\varrho}_c$ as a function of ϱ_s. Thus, $\tilde{\varrho}_c(0)$ is the amount of C on the strand in the absence of S's, while $\tilde{\varrho}_c(\varrho_s)$ is the amount of C's on the strand with the indicated amount of S put in solution. With this taken into account the quenching is given by

$$\text{quenching} \equiv \frac{I_0}{I} = \frac{\tilde{\varrho}_c(0)}{\tilde{\varrho}_c(\varrho_s)}\left[1 - \frac{\gamma_1[R - \alpha(R-1)]}{1 - \alpha(1-\gamma_1)}\right]^{-2} \tag{6.6}$$

with γ_1 given by (6.3), where the densities in the expression for γ_1 are $\tilde{\varrho}_s$ and $\tilde{\varrho}_c$, as given in (6.4).

7. Fitting Experimental Data. The steady state luminescence quenching experiments between $[Ru(phen)_2(dppz)]^{2+}$ and $[Rh(phi)_2(phen)]^{3+}$, both bound on calf thymus DNA, revealed distinctly upward curving Stern–Volmer plots.[3]

For the experimental system consisting of 1000 μM CT-DNA (in phosphate units, bases, not base pairs), 10 μM $[Ru(phen)_2(dppz)]^{2+}$ as photosensitizer, and 0–100 μM $[Rh(phi)_2(phen)]^{3+}$ as electron acceptor, a factor 10 decrease in the integrated luminescence intensity was observed, whereas the time-resolved laser flash experiment showed only changes in the excited state lifetimes of less than a factor of 3. To demonstrate the abilities of our model to describe DNA-mediated electron transfer, we fitted the data from this quenching experiment employing $[Ru(phen)_2(dppz)]^{2+}$ and $[Rh(phi)_2(phen)]^{3+}$ on CT-DNA.[3] The structures involved in the experimental system are shown in

TABLE 1: Experimental Data Used

Calf Thymus (10^4-mer)[20]		
Rh (μM)	ϱ_s	I_0/I
0.00	0.0000	1.000
9.95	0.0796	1.288
19.80	0.1584	1.590
29.56	0.2365	2.038
39.22	0.3138	2.574
48.78	0.3902	3.416
58.25	0.4660	3.970
67.63	0.5410	4.246
76.92	0.6154	6.238
86.12	0.6890	7.254
95.24	0.7619	8.669

Figure 1. The data to be fit involve metalocomplexes bound to calf thymus DNA and are given in Table 1.

There are three parameters involved in the fits. The quantity R measures interaction of the two kinds of complex. $R > 1$ represents attraction, $R < 1$ repulsion. The physically most plausible situation is $R = 1$ or slightly less than 1 (because both complexes are positively charged). Below we give best fits for several R values, including $R > 1$, although the latter is provided mainly to bound our most conservative estimates for the electron transfer length. The second parameter is ϱ_∞, representing a saturation effect in the capacity of the DNA to absorb complexes at high loading. Because of the high affinity, we have an a priori preference for $\varrho_\infty \approx \varrho_{\text{jamming}} \approx 0.08$; however, the fits were best for higher values. This suggests that for extremely high loading further nonlinear terms in eq 3.1 would be required. Finally, the central object of our investigation is L, the electron transfer range, in this article measured in units of 4 base pairs with the zero of L beginning at the *next*-nearest neighbor. (In the other words, $L = 1$ corresponds to 4 + 4 base pairs for the center-to-center distance.)

The fit proceeded as follows: A value of R was fixed and ϱ_∞ and L adjusted so as to minimize a weighted least squares distance of the data points from the function given in eq 6.6 (with appropriate functional dependence of its parameters on ϱ_∞ and L as described by prior equations in section 6). The weighting gave less importance to high loading values, as the error bars on these points were considered to be larger. In Figure 2 the solid line shows the fit to the data with $R = 1$, $L = 0.792$, and $\varrho_\infty = 1.7668$. In fact the sensitivity to ϱ_∞ is slight for low values of ϱ_s. This is evident from the dotted curve in the same figure, which uses $\varrho_\infty = 15$ and the other parameters unchanged. This is a reasonable result, inasmuch as ϱ_∞ corrects high loading saturation effects.

Sensitivity to L is more significant. In Figure 3 we show attempts to fit the data with L values greater and smaller by 0.2 than the best value given above (and used in Figure 2). In each case ϱ_∞ was optimized for the given L. The fit is markedly inferior to that in Figure 2 and in particular cannot accommodate fairly reliable low loading values. (Forcing such accommodation causes large errors at high loading (the latter is not shown).)-

When other R values are used, it is still possible to vary L and ϱ_∞ so as to get good fits. The optimal values are given in Table 2. In Figure 4 we show *all* such curves, superimposed on one another. There is evidently no basis for preference of one data set over another based on the appearance of the graph alone. The numerical optimization showed a slight preference, in that the figure of merit—the weighted least squares difference—was slightly smaller for $R = 0.9$ and $R = 1.0$.

Conclusion

In this report we present a model for the quantitative description of electron transfer quenching involving photoexcited

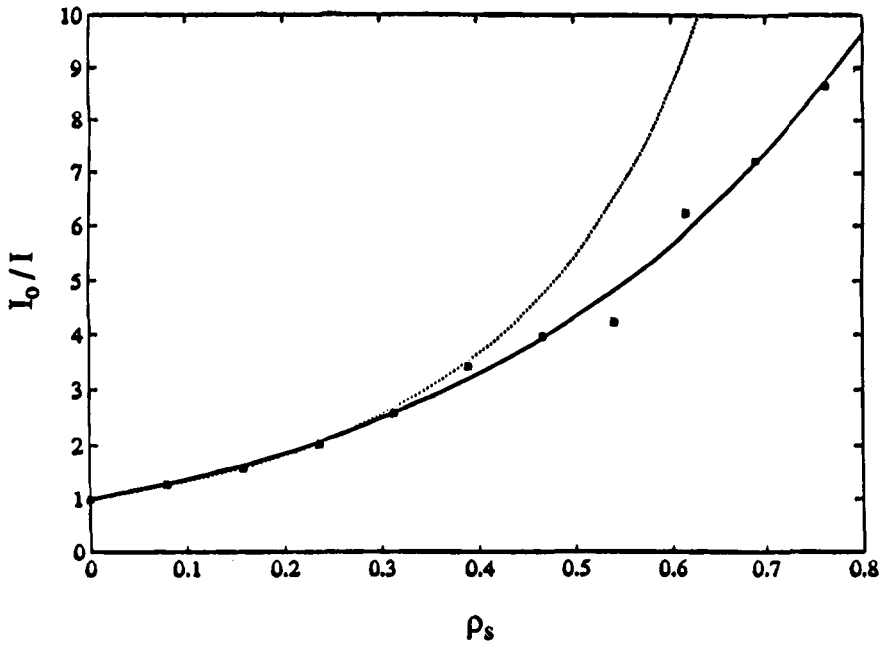

Figure 2. Fit of the calf thymus data with $R = 1$ and $L = 0.792$. The solid line corresponds to the optimal value of ϱ_∞, namely, 1.7668, while the dotted line represents $\varrho_\infty = 15$.

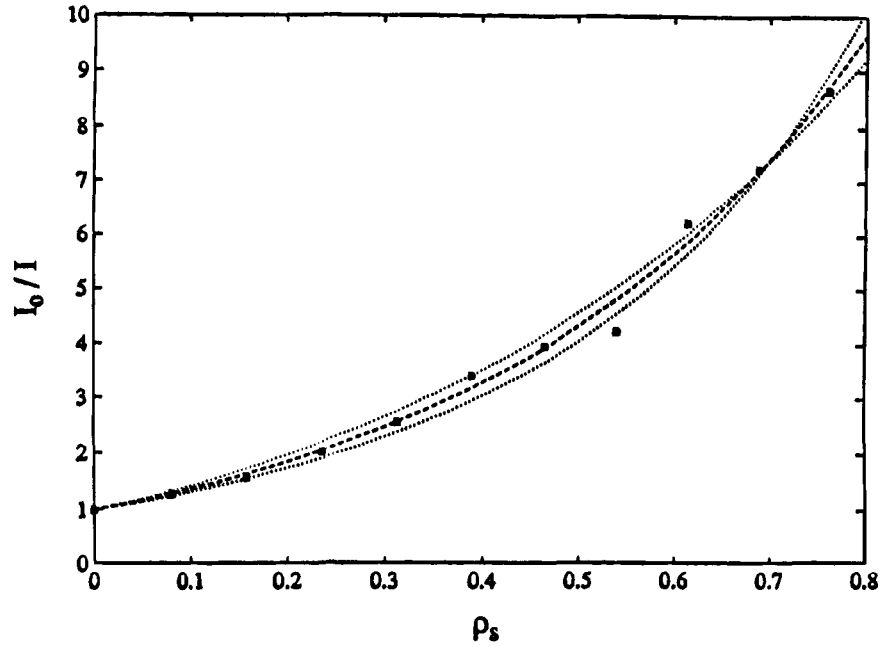

Figure 3. Effect on the data fit due to varying L (with $R = 1$). The dashed line is the same as the solid line for Figure 2. The dotted lines are for L taken 0.2 above and below the optimal values. The value of ϱ_∞ is optimized for those values.

TABLE 2: Optimal L and ϱ_∞ for Various Values of R

R	L	ϱ_∞
0.8	1.0516	2.6792
0.9	0.9234	2.1257
1.0	0.7917	1.7677
1.1	0.6543	1.5161
1.2	0.5044	1.3298

metal complexes both as electron donors and electron acceptors and with both bound to DNA. The model takes a phenomenological approach, treating both random and correlated deposition of the metal complexes on DNA, the inclusion of correlations being the appropriate course for accommodating attraction or repulsion between the complexes. Furthermore, our model allows displacement of donor molecules from the DNA, although with minor changes the no-displacement situation can also be treated. Finally, we include the effects of incomplete binding of the complexes to the DNA, a significant effect at high donor and acceptor concentrations.

The model has been used to fit experimental data using calf thymus DNA, $[Ru(phen)_2(dppz)]^{2+}$ as photoelectron donor, and $[Rh(phi)_2(phen)]^{3+}$ as electron acceptor.

The results of our computations indicate that DNA can be regarded as a supporting medium for relatively long range electron transfer. The calculation of the interaction length L from our model on the basis of our experimental data and assuming an exponential drop-off of the interaction between donor and acceptor leads to a value of 24 Å for the center-to-center transfer distance. This is based on a distance between base pairs on a DNA double strand B-DNA of approximately 3.4×10^{-10} (m).[1f] From Figure 3, we deduce that our fit has

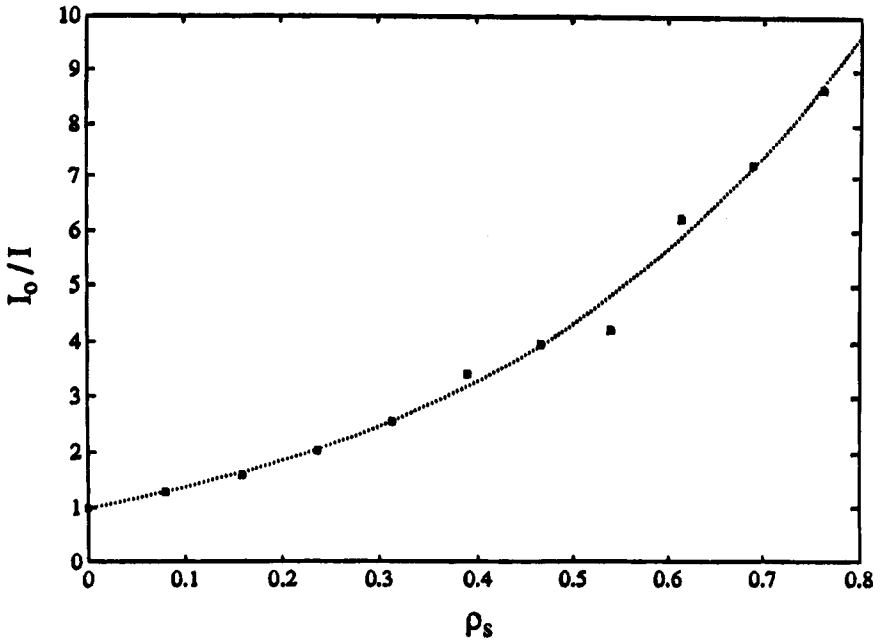

Figure 4. Fits for *all R* values given in Table 2, superimposed on one another. (The curves lie atop one another to the precision of the printer.)

significance at the level of about 1 base pair, which is also the limit imposed on our calculation from the ignoring of fine distance gradations, as discussed in section 3, above. Furthermore, even if we were to assume an unrealistic supramolecular interaction between donor and acceptor molecules, the range would only be reduced by about 1 base pair. (See Table 2.) Recall from section 4 that the parameter $R \equiv \gamma_0/\gamma_1$ describes attraction or repulsion between the photodonor and electron acceptor metal complexes (circles and squares in our notation). Thus, for $R = 1.1$ there would be a 10% increase in the likelihood that a site adjacent to a C would be occupied (by an S) compared to the likelihood of a nonadjacent site being occupied.) The relatively long value (24 Å) for the transfer distance is consistent with other recent information[18] and with new theoretical conduction band models that have been developed.[19]

We close by commenting on how relaxation of some assumptions would affect the calculated range of electron transfer. For example, if intervening circles *did* block the quenching effect of squares, we would have required *larger* values of L to achieve the same quenching. The no-displacement assumption is probably neutral with respect to estimating L. Implicit in eq 2.2 is the assumption that for distance "zero" (adjacency) quenching is complete. Relaxing this would require larger L. (Note, by the way, that our quoted 24 Å is not the range for the exponent in eq 2.2 It is that range, as given in Table 2, plus 4 base pairs, representing the finite size of the complex. Thus the drop-off parameter for more distant squares is $L \approx 0.79$, or about 11 Å.) We have also included $R > 1$ data, despite the fact that we do not believe there to be net attraction between the complexes, to show how seriously that might affect our estimates. Finally, the use of ϱ_∞ values larger than $\varrho_{\text{jamming}} \approx 0.8$ represents an Occam's razor guided phenomenology. For high affinity one should seldom find on-strand densities greater than ϱ_{jamming}. This could be handled by including nonlinear terms in the denominator of eq 3.1, but an additional parameter is undesirable and the fits are good as they stand. It is interesting that even if one forces $\varrho_\infty = \varrho_{\text{jamming}}$, the value of L does not change significantly. One gets $L = 1.25$ (so we are again being conservative in that this would increase our range by about 2 base pairs), but the fit, while not unreasonable, is not quite so good as that given by the larger values of ϱ_∞.

Acknowledgment. We are grateful to Claudia Turro for her help in preparing this work. The data used in the calculations were provided by Michelle R. Arkin and Jaqueline K. Barton, and we are happy to acknowledge this contribution. We thank the National Science Foundation (PHY 93 16681 to L.S.S. and CHE 90 14817 to N.J.T.) and the Air Force Office of Scientific Research (to N.J.T.), as well as the Deutsche Forschungsgemeinschaft (to S.H.B.) for their generous financial support.

References and Notes

(1) Marcus, R. A.; Sutin, N. *Biochim. Biophys. Acta* **1985**, *811*, 265. Bowler, B. E.; Raphael, A. L.; Gray, H. B. *Prog. Inorg. Chem.* **1990**, *38*, 259. Wang, J. C.; Giaver, G. N. *Science* **1988**, *240*, 300. Porschke, D. *Biophys. Chem.* **1991**, *40*, 169. Fried, M. G.; Crothers, D. M. *J. Mol. Biol.* **1984**, *172*, 263. Saenger, W. *Principles of Nucleic Acid Structure*; Springer-Verlag: New York, Berlin, Heidelberg, London, Paris, Tokyo, 1988; p 556.

(2) Hoffmann, T. A.; Ladik, J. *Adv. Chem. Phys.* **1964**, *7*, 84. Dee, D.; Bauer, M. E. *J. Chem. Phys.* **1974**, *60*, 541. Clementi, E.; Corongiu, G. *Int. J. Quantum Chem. Quantum Biol. Symp.* **1982**, *9*, 213.

(3) Murphy, C. J.; Arkin, M. R.; Ghatlia, N. D.; Bossmann, S. H.; Turro, N. J.; Barton, *Proc. Natl. Acad. Sci.* **1994**, *91*, 5315–5319.

(4) Friedman, A. E.; Chambron, J.-C.; Sauvage, J.-P.; Turro, N. J.; Barton, J. K. *J. Am. Chem. Soc.* **1990**, *112*, 4960. Friedman, A. E.; Kumar, C. V.; Turro, N. J.; Barton, J. K. *Nucleic Acids Res.* **1991**, *19*, 2595. Hartshorn, R. M.; Barton, J. K. *J. Am. Chem. Soc.* **1992**, *114*, 5919. Jenkins, Y.; Friedman, A. E.; Turro, N. J.; Barton, J. K. *Biochemistry* **1992**, *31*, 10809. Sitlani, A.; Long, E. C.; Pyle, A. M.; Barton, J. K. *J. Am. Chem. Soc.* **1992**, *114*, 2303. Uchida, K.; Pyle, A. M.; Morii, T.; Barton, J. K. *Nucleic Acids Res.* **1989**, *17*, 10259.

(5) McGhee, J. D.; Hippel, P. H. v. *J. Mol. Biol.* **1974**, *86*, 469.

(6) Dong, Y.; Shao, W.; Tang, W.; Dai, A. *Huaxue Xuebao* **1991**, *49*, 1478–1482. Matai, S.; Bhattacharya, K. L. *Indian J. Biochem. Biophys.* **1986**, *23*, 197–203. Gaugain, B.; Barbet, J.; Capelle, N.; Roques, B. *Biochemistry* **1978**, *14*, 5078–5088.

(7) Purugganan, M. D.; Kumar, C. V.; Turro, N. J.; Barton, J. K. *Science* **1988**, *241*, 1645. Orellana, G.; Mesmaeker, A. K.-D.; Barton, J. K.; Turro, N. *J. Photochem. Photobiol.* **1991**, *54*, 499.

(8) CT-DNA was purchased from SIGMA and carefully dialyzed against 1.0 mM Trizma-buffer.

(9) Friedman, A. E.; Turro, N. J.; Barton, J. K. In *Fifth International Conference on Bioinorganic Chemistry (ICBIC-5)*; Oxford University Press: Oxford, U.K., 1991; p 442.

(10) In the case that a C is considered to block the effect of an S–C pair on either side of it, we must consider also the possibility that there is

a C to the left or right that is closer than the S. We will not go into this, but will quote the result below.

(11) The time for reaching equilibrium using the strong intercalator $[Ru(phen)_2(dppz)]^{2+}$ under our experimental conditions we estimate to be 1−6 h depending on the DNA/complex ratio: Bossmann, S. H.; Turro, C.; Schulman, L. S.; Turro, N. J. To be published.

(12) Gonzales, J. J.; Hemmer, P. C.; Høye, J. S. *Chem. Phys.* **1974**, *3*, 228.

(13) Nielaba, P.; Privman, V. P. *Mod. Phys. Lett. B* **1992**, *6*, 533. Privman, V.; Wang, J. S.; Nielaba, P. *Phys. Rev. B* **1991**, *43*, 3366.

(14) Schneider, H.-J.; Theis, I. *Angew. Chem., Int. Ed. Engl.* **1989**, *28*, 753.

(15) The same binding constant for S's and C's was considered in all cases.

(16) Thompson, C. J. *Mathematical Statistical Mechanics*; MacMillan: New York, 1972.

(17) The formation of B from C and S is considered to be an equilibrium reaction with the considerations of the present section.

(18) Murphy, C. J.; Arkin, M. R.; Jenkins, Y.; Ghatlia, N. D.; Bossmann, S. H.; Turro, N. J.; Barton, J. K. *Science* **1993**, *262*, 1025.

(19) Felts, A. K.; Pollard, W. T.; Friesner, R. A. *J. Phys. Chem.*, in press.

(20) The intensity data were calculated from the decay traces in the time-resolved laser experiments. A conservative estimation of the error in these measurements leads to ±10 rel %.

JP942566D